

# Mitigating Ferranti Effect and Enhancing Transmission Line Efficiency through Shunt Reactor Placement in Remote Grids

Hanan H. Kashef  
General Court, Egyptian Electricity  
Transmission Company  
Egyptian Ministry of Electrical and  
Renewable Energy  
Cairo, Egypt  
hanan1.hamdy@f-eng.tanta.edu.eg

Rabah Y. Amer  
Electrical Power and Machines Dept.  
Faculty of Engineering,  
Cairo University  
Cairo, Egypt  
rabah\_amer@yahoo.com

Mohamed K. El-Nemr,  
Ahmed M. Omara  
Electrical Power and Machines Dept.  
Faculty of Engineering,  
Tanta University  
Tanta, Egypt  
melnemr@f-eng.tanta.edu.eg  
ahmed.omara@f-eng.tanta.edu.eg

**Abstract**—This paper addresses the mitigation of the Ferranti effect and the enhancement of high-voltage long transmission line performance and reliability through strategic shunt reactor placement and sizing. The study presents a comprehensive analysis of shunt reactor selection for a section of the power system featuring interconnected high-voltage long transmission lines, using real-world data from the New Valley Governorate, Egypt, collected by the Egyptian Transmission Company. Through simulations using the Electromagnetic Transient and Analysis Program (ETAP), we determine the minimal reactor requirements for satisfactory performance, considering various loading conditions and allocation proposals.

The results show effective Ferranti effect mitigation, improved system reliability, reduced potential for blackouts, and enhanced transmission line efficiency. This research provides a valuable solution that reduces costs, enhances system safety and performance, and has been validated through practical field measurements. It contributes to optimizing shunt reactor placement in remote grid configurations, benefiting overall power system efficiency and resilience. A variety of simulations have been executed, providing essential insights into the optimal deployment of reactors to enhance voltage stability and system reliability across diverse operational scenarios.

**Keywords**—*Electromagnetic Transient and Analysis Program (ETAP)*, *Ferranti effect*, *high-voltage transmission lines*, *reliability*, *shunt reactor*, *system performance optimization*.

## I. INTRODUCTION

The installation of shunt reactors on high-voltage long transmission lines represents a standard solution aimed at mitigating the adverse effects of the Ferranti effect, particularly during light loading conditions. The Ferranti effect, characterized by over-voltage conditions, poses a considerable risk to power equipment, including its potential to induce equipment damage and failure due to increased stress on insulation systems. It is well-established in the literature that transmission line capacitance is inherently dependent on its length, resulting in capacitive load conditions on long transmission lines during light loading. This, in turn, may lead to a scenario where the receiving end voltage surpasses the sending end voltage, a phenomenon commonly referred to as the Ferranti effect [1].

To counteract these adverse effects and ensure the reliable operation of high-voltage long transmission lines, the installation of shunt reactors has become imperative. The selection process for these reactors, encompassing both size and location, emerges as a critical factor, particularly in interconnected long transmission line configurations [2].

While the need for interconnected high-voltage long transmission lines is relatively rare, such configurations are essential for connecting remote regions, such as distant cities and oases deep within arid deserts [3].

The management of voltage fluctuations between sending and receiving ends in the electrical system is crucial for ensuring operational stability and power quality. Compensation techniques have been employed to address these voltage variations, particularly when voltage levels exceed the required limits, which are determined by the reactive power balance in the system. Two primary compensation types, namely active and passive, are discussed.

Active compensation techniques leverage FACTS (Flexible AC Transmission Systems) technology to enhance voltage control and power transfer capability, offering improved controllability of the power system [4]–[6]. FACTS technology aligns with the objective of controlling power flow over designated transmission routes. Within the active compensation category, two key components are highlighted:

As a member of the FACTS family, Static Var Compensator (SVC) plays a vital role in injecting or absorbing reactive power to enhance dynamic performance and transient stability of the power system. It uses electronic switching devices to control voltage and power flow, ultimately improving voltage regulation and system loss reduction [5]–[7].

Static Synchronous Compensator (STATCOM) is a fast-acting device capable of providing or absorbing reactive current, thereby regulating voltage at the point of connection to the power grid. It falls under the category of FACTS devices and significantly improves voltage profiles and reduces power losses in transmission systems [3].

Within the passive compensation category, shunt reactors play a critical role in inductive reactive power compensation. They positively impact system stability, economy, and line transmission capacity [5], [6], [8]. Shunt reactors are instrumental in absorbing excess capacitive reactive power during periods of low load operation, effectively controlling voltage levels [2]. In situations where long and high-voltage transmission lines experience light loading conditions, the excess reactive power associated with the Ferranti Effect can be absorbed by shunt reactors, preventing voltage instability [9]. Additionally, variable shunt reactors (VSRs) are introduced as a dynamic solution, allowing for fine-tuning of voltage in the system and efficient compensation for varying load conditions.

The effectiveness of these compensation techniques in managing voltage fluctuations and enhancing system stability makes them integral components in modern power transmission systems. Active and passive compensation methods provide the necessary tools to address voltage control challenges and maintain optimal power quality in the electrical network.

Through extensive simulations, encompassing various loading conditions and allocation proposals for shunt reactors, this study aims to determine the minimum reactor requirements necessary to ensure satisfactory performance, considering both the number and capacity of these reactors. Additionally, the research delves into defining the voltage boundaries that delineate regions of satisfactory performance. It is essential to note that the benefits extend beyond Ferranti effect mitigation. The outcomes of this research highlight an appreciable enhancement in overall system reliability, a reduction in potential blackouts, and an improvement in transmission line efficiency, thereby enhancing the overall system efficiency [10].

This study focuses on presenting a comprehensive analysis of the selection process for shunt reactors in terms of size and location, targeting a section of the power system that features interconnected high-voltage long transmission lines. The research employs actual parameters and load data gathered by the Egyptian Transmission Company to model and simulate an extensive network, encompassing over twenty stations connected by high-voltage long transmission lines. The simulation leverages the Electromagnetic Transient and Analysis Program (ETAP), a widely recognized software tool for power system studies.

This paper provides detailed insights into system configuration, parameters, and performance for diverse scenarios. Moreover, the results are meticulously compared

with practical field measurements, demonstrating the reasonable accuracy of the developed simulation results. In conclusion, this study offers a proposed solution characterized by minimal size and suitability for selected locations, thereby augmenting system safety, reliability, and performance, while also reducing initial costs and operational expenses.

The paper is organized into four sections, covering the power system description, modes of operation, system simulations, and analysis, and concluding with the key findings and recommendations.

## II. POWER SYSTEM DESCRIPTION

### A. Southern Zone of Egypt's Electrical Grid

The system under consideration is a component of an Egyptian electrical transmission company located in the southern region. It comprises a single generator stationed at the High-Dam Busbar, in addition to two 500 kV Busbars, interconnected with 220 kV Busbars via transformers.

To manage voltage levels and ensure system stability, a total of ten reactors have been strategically installed on all four Busbars. These reactors are equipped with supports that facilitate their seamless connection and disconnection with the conductors. Their primary function is to mitigate the occurrence of high voltages on the extensive transmission line, particularly when the load is reduced to its minimum.

The map provides a visual representation of the considerable distances separating the various stations within the southern zone of Egypt's electrical grid as shown in Fig. 1. It illustrates the energy transmission route originating from High-Dam, which feeds power into the Nagaa Hammady station (500 kV), subsequently distributing electricity to other stations. The longest stretch of transmission lines, denoted in red font, is the line connecting the Owainat and Balat stations, spanning a distance of 420 kilometers. This data is further

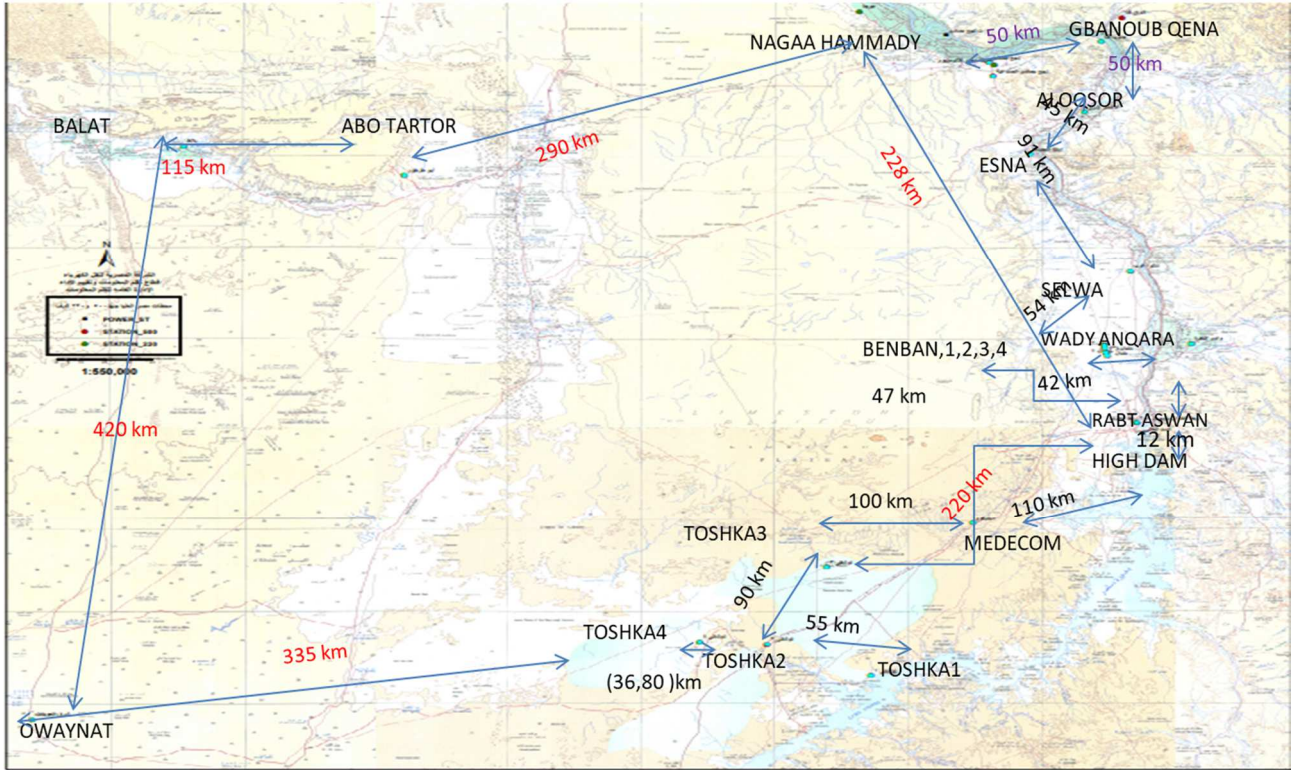


Fig. 1. Geographical Distances Between Stations in Egypt's Southern Electrical Grid Sector.

elaborated in the table detailing the electrical transmission line configurations.

### B. Electrical Transmission Line Data

The data pertaining to electrical transmission lines follows an incremental section type distribution. These precise parameters have been obtained through measurements conducted by the Ministry of Electricity, employing a meticulous approach to eliminate any discrepancies resulting from sag effects. Consequently, the provided data represents the actual impedance characteristics for all lines within the examined system. The TABLE I showcases line specifications, including distance between stations as simulated by busbar, as well as the positive, negative, and zero impedance values associated with the lines.

### C. System Configuration and Reactor Placement

The Single Line Diagram (SLD), as illustrated in Fig. 2, provides a comprehensive visual representation of the station configuration within the 500 kV and 220 kV busbars, showcasing the positioning of the generator at High-Dam and the strategic installation of reactors within the system at

specific busbars. This diagram serves as a valuable reference point for understanding the structural layout of the station and the critical components integrated into the electrical transmission system.

Within the system, these reactors have been strategically placed with high voltage circuit breakers on all four busbars, each accommodating two conductors. The inclusion of supports enables the seamless connection and disconnection of these reactors, contributing to the flexibility and adaptability of the system. The relevant details pertaining to the circuit breakers and reactors, including their names, their respective positions as the first and last elements in the transmission line, and the capacity of each reactor within the system, are meticulously documented in the accompanying TABLE II. This table serves as a comprehensive reference, providing essential information about the key components and their roles within the electrical transmission system, enhancing the overall understanding of its functionality and design.

TABLE I. IMPEDANCE CHARACTERISTICS OF ELECTRICAL TRANSMISSION LINES IN THE STUDIED SYSTEM

| FROM STATION (Loading) | TO STATION (Loading) | LENGTH (KM) | Positive & Negative impedance |                |                | Zero impedance |                |                |
|------------------------|----------------------|-------------|-------------------------------|----------------|----------------|----------------|----------------|----------------|
|                        |                      |             | R ( $\Omega$ )                | X ( $\Omega$ ) | Y ( $\Omega$ ) | R ( $\Omega$ ) | X ( $\Omega$ ) | Y ( $\Omega$ ) |
| Toshka 2 (30 MW)       | Toshka 1 (72.5 MW)   | 55          | 0.0412                        | 0.302          | 3.72           | 0.11           | 0.95           | 2.23           |
| Toshka 2 (30 MW)       | Toshka 3 (130 MW)    | 90          | 0.0412                        | 0.302          | 3.72           | 0.11           | 0.95           | 2.23           |
| Toshka 2 (30 MW)       | Benban 3             | 280         | 0.0217                        | 0.295          | 3.96           | 0.247          | 0.78           | 2.92           |
| Toshka 3 (130 MW)      | Medecom (10 MW)      | 100         | 0.4118                        | 0.302          | 1.184          | 0.02273        | 0.19628        | 0.10793        |
| Toshka 3 (130 MW)      | High dam             | 220         | 0.412                         | 0.302          | 3.72           | 0.011          | 0.95           | 2.23           |
| Medecom (10 MW)        | High dam             | 110         | 0.0412                        | 0.302          | 3.72           | 0.11           | 0.95           | 2.23           |
| High dam               | Rabt aswan (308 MW)  | 12          | 0.0412                        | 0.302          | 3.72           | 0.011          | 0.95           | 2.23           |
| Rabt aswan (308 MW)    | Wady naqra (88 MW)   | 67          | 0.0412                        | 0.302          | 3.72           | 0.011          | 0.95           | 2.23           |
| Wady naqra (88 MW)     | Benban 4             | 42          | 0.0412                        | 0.302          | 3.72           | 0.011          | 0.95           | 2.23           |
| Benban4                | Benban3              | 2           | 0.0412                        | 0.302          | 3.72           | 0.011          | 0.95           | 2.23           |
| Benban3                | Benban 2             | 3           | 0.04223                       | 0.3159         | 3.622          | 0.2463         | 1.016          | 2.1138         |
| Benban2                | Benban 1             | 2           | 0.0412                        | 0.302          | 3.72           | 0.11           | 0.95           | 2.23           |
| Benban 1               | Selwa (170 MW)       | 54          | 0.0412                        | 0.3159         | 3.622          | 0.2463         | 1.0163         | 2.11388        |
| Selwa (170 MW)         | Esna (44.5 MW)       | 91          | 0.0412                        | 0.302          | 3.72           | 0.11           | 0.95           | 2.23           |
| Esna (44.5 MW)         | Aloqsor (368 MW)     | 45          | 0.0412                        | 0.302          | 3.72           | 0.11           | 0.95           | 2.23           |
| Aloqsor (368 MW)       | Ganob qena (348 MW)  | 50          | 0.0412                        | 0.302          | 3.72           | 0.11           | 0.95           | 2.23           |
| Ganob qena (348 MW)    | Alsenaeaya (294 MW)  | 50          | 0.0412                        | 0.302          | 3.72           | 0.11           | 0.95           | 2.23           |
| High dam               | Alsenaeaya (294 MW)  | 228         | 0.0217                        | 0.302          | 3.96           | 0.247          | 0.845          | 2.92           |
| Toshka 4 (330 MW)      | Toshka 2 (30 MW)     | 36          | 0.0412                        | 0.302          | 3.72           | 0.11           | 0.95           | 2.23           |
| Owainat (141 MW)       | Toshka 4 (330 MW)    | 80          | 0.0412                        | 0.302          | 3.72           | 0.11           | 0.95           | 2.23           |
| Balat (52 MW)          | Abo tartor (76 MW)   | 335         | 0.0412                        | 0.302          | 3.72           | 0.11           | 0.95           | 2.23           |
| Abo tartor (76 MW)     | Alsenaeaya (294 MW)  | 115         | 0.0412                        | 0.302          | 3.72           | 0.11           | 0.95           | 2.23           |
|                        |                      | 290         | 0.0835                        | 0.418          | 2.85           | 0.3            | 0.95           | 2.23           |

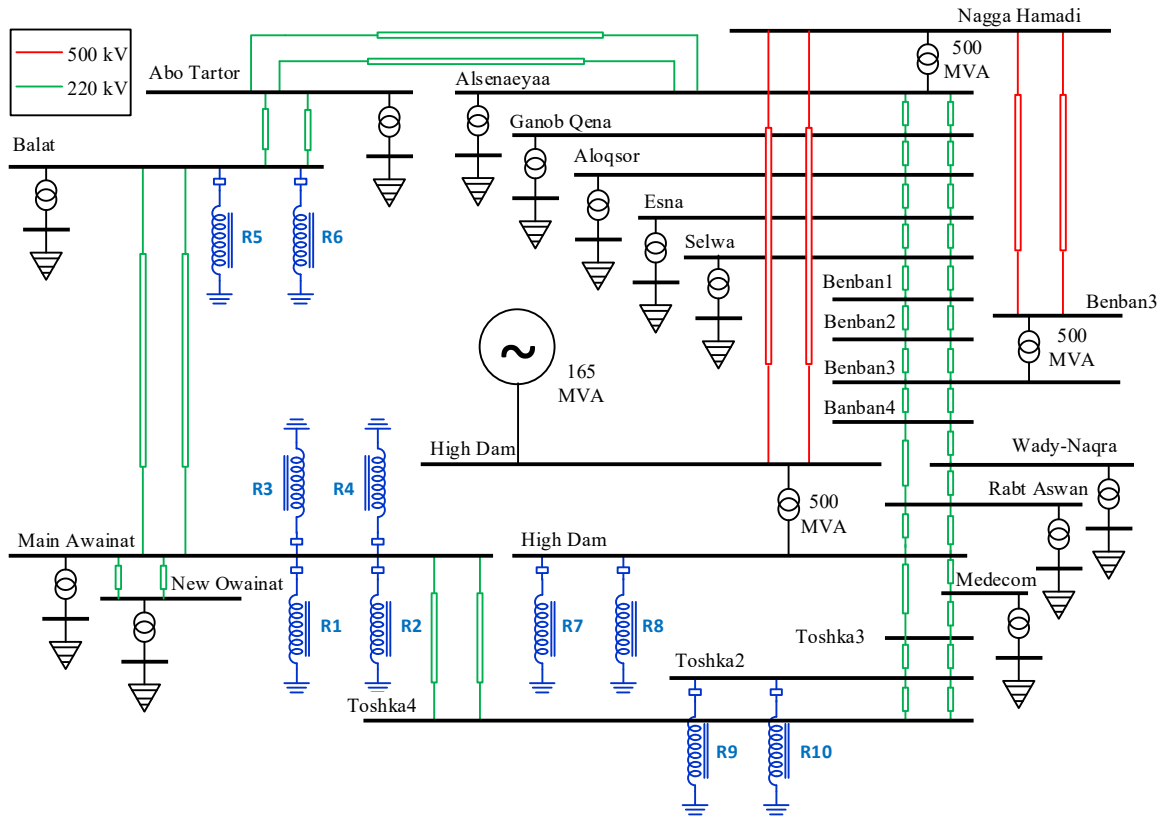


Fig. 2. Single Line Diagram (SLD) of 500 KV and 220 KV Stations with Reactor Placement.

### III. MODES OF OPERATION AND LOADING CONDITIONS

In the current operational spectrum, the electrical transmission system is subject to various distinct modes, each characterized by specific load conditions that influence its performance and reliability.

#### A. Present Operation Modes

1) *Full Load Condition*: This mode represents the system's highest load capacity, where it operates at its maximum designed capacity, ensuring the efficient and effective transmission of electrical power.

2) *Half Load Condition*: Under this mode, the system carries a load equal to half of its maximum capacity. It operates with reduced load demands, providing a level of flexibility to accommodate varying power requirements.

3) *Minimum Load (65%)*: The system also operates under minimum load conditions, which correspond to approximately 65% of the operation voltage, as determined from daily loading data recorded by the electrical ministry.

This mode accounts for periods of low power demand, optimizing resource allocation.

4) *No Load Condition*: In this mode, the system operates with no electrical load. It represents a state of minimal power consumption, typically occurring during maintenance or low-demand periods.

#### B. Modes of Growth Loading in the Future

As the system anticipates future increases in power demand, various growth loading modes have been considered to ensure its adaptability and scalability.

1) *+5% Growth Load from Full Load*: This mode envisions a 5% increase in power demand from the system's current full load operation. It prepares the system to accommodate gradual growth in electrical consumption.

2) *+10% Growth Load from Full Load*: In anticipation of a 10% increase in power demand from the current full load operation, this mode provides a more substantial buffer to manage heightened load conditions effectively.

3) *+15% Growth Load from Full Load*: This mode plans for a 15% increase in power demand from the current full load operation, reflecting a significant uptick in electrical consumption.

4) *+20% Growth Load from Full Load*: The most robust growth loading mode, this configuration prepares the system to handle a 20% increase in power demand from the current full load operation, ensuring its resilience and adaptability in the face of substantial load growth.

These operation modes and growth loading scenarios are pivotal in assessing the system's capacity to meet future energy demands while maintaining stability and reliability.

TABLE II.  
REACTORS LOCATIONS IN THE ELECTRICAL  
TRANSMISSION SYSTEM

| Reactor No. | C.B No. | From Busbar – To Busbar | CAPACITY (MVA) |
|-------------|---------|-------------------------|----------------|
| R1          | A       | Owainat-toshka 4        | 25             |
| R2          | B       | Owainat-toshka 4        | 25             |
| R3          | C       | Owainat-balat           | 25             |
| R4          | D       | Owainat-balat           | 25             |
| R5          | F       | Balat-owainat           | 25             |
| R6          | E       | Balat-owainat           | 25             |
| R7          | K       | High dam -alsenaeya     | 165            |
| R8          | G       | High dam-alsenaeya      | 165            |
| R9          | M       | Toshka 2-toshka 3       | 25             |
| R10         | L       | Toshka 2-toshka 3       | 25             |

They form the basis for critical decision-making processes in power system management and infrastructure planning.

### C. Existing Voltage Stabilization through Reactor Integration

The connection of reactors within the system plays a crucial role in regulating and maintaining the voltage balance across the busbars. The daily readings shown in TABLE III, obtained from actual measurements at various times, provide clear evidence that these reactors effectively adjust voltage levels when they tend to deviate from their prescribed values. By strategically connecting and disconnecting the reactors as needed, the system can counteract high voltage conditions, thereby ensuring that the busbars operate within the specified voltage limits. This voltage regulation function of the reactors not only enhances the stability and reliability of the electrical transmission system but also contributes significantly to maintaining power quality and ensuring the smooth flow of electricity through the network. The data illustrates that the voltage exhibits variation within a 6.8% range of the nominal 220KV, while the reactor effectively fine-tunes the voltage level in response.

## IV. SYSTEM SIMULATION AND ANALYSIS

The simulation and analysis of the obtained results were conducted studiously using the ETAP program, a robust tool employed to model and analyze the electrical transmission system. The primary objectives of this simulation were to comprehensively evaluate the load flow and voltage profiles across the busbars under various operating conditions. These conditions encompassed different modes of operation and distinct reactor connection scenarios.

In the analysis, a critical consideration was the tolerance ratio of  $\pm 10\%$  relative to the operation voltage of 220KV. This tolerance range derived from the rated voltage and the tapping

TABLE III. DAILY READING OF BUSBAR VOLTAGES WHILE REACTORS ARE CONNECTED

| Time (HR) | Busbar Voltage (KV) | Toshka1         | Toshka2 | Balat1 | Balat2 |
|-----------|---------------------|-----------------|---------|--------|--------|
|           |                     | Power load (MW) |         |        |        |
| 1:00      | 222                 | 39              | 39      | 14     | 14     |
| 2:00      | 223                 | 39              | 39      | 16     | 16     |
| 3:00      | 225                 | 38              | 38      | 14     | 14     |
| 4:00      | 228                 | 38              | 38      | 12     | 12     |
| 5:00      | 223                 | 38              | 38      | 6      | 6      |
| 6:00      | 221                 | 37              | 37      | 8      | 8      |
| 7:00      | 218                 | 39              | 39      | 16     | 16     |
| 8:00      | 215                 | 45              | 45      | 26     | 26     |
| 9:00      | 220                 | 56              | 56      | 20     | 20     |
| 10:00     | 219                 | 55              | 55      | 40     | 38     |
| 11:00     | 213                 | 57              | 57      | 38     | 40     |
| 12:00     | 214                 | 55              | 55      | 40     | 42     |
| 13:00     | 215                 | 55              | 55      | 42     | 42     |
| 14:00     | 214                 | 56              | 56      | 42     | 42     |
| 15:00     | 219                 | 55              | 55      | 42     | 40     |
| 16:00     | 214                 | 58              | 58      | 40     | 39     |
| 17:00     | 219                 | 56              | 56      | 36     | 28     |
| 18:00     | 221                 | 47              | 47      | 18     | 18     |
| 19:00     | 220                 | 43              | 43      | 18     | 14     |
| 20:00     | 220                 | 43              | 43      | 14     | 14     |
| 21:00     | 220                 | 43              | 43      | 12     | 14     |
| 22:00     | 221                 | 43              | 43      | 14     | 14     |
| 23:00     | 222                 | 38              | 38      | 14     | 14     |
| 24:00     | 224                 | 38              | 38      | 12     | 14     |

range, which is specified as 220KV with an allowable variation of  $\pm 8\%$  (equivalent to 1.25% per step). The ETAP program proved instrumental in accurately calculating the busbar voltage values via load flow calculations, providing a comprehensive insight into the system's behavior.

The analytical framework was structured into two fundamental segments: one examining the system without the integration of reactors and the other assessing the system with reactors in place. These evaluations were conducted across diverse operational modes, allowing for a thorough comparison of voltage profiles and load flow characteristics. The results derived from this comprehensive simulation and analysis process are instrumental in informing critical decisions regarding the system's performance and its ability to maintain voltage stability across varying operational scenarios.

### A. Present Operation Modes without Reactors

Different loading conditions are simulated without reactors as shown in Fig. 3 and analyzed as follows:

1) *Full Load without reactors*: In the Full Load mode as shown in Fig. 3, it is evident that the voltages across all buses remain within acceptable limits, not exceeding 100% of the rated voltage value. As a result, there is no necessity for the installation of any reactors. However, certain stations, such as Ganob Qena, Esna, and Aloqsor, exhibit voltages that fall below 90% of the operational value, which is below the tolerance range of  $\pm 10\%$  from the operational value. In these instances, capacitors must be connected to elevate the voltage to levels compliant with operational standards. The voltage ratios at these stations are notably low without the inclusion of reactors, emphasizing the need to employ capacitance to raise the voltage ratio to reach 100% of the rated value. Parallel capacitor banks are employed to mitigate losses and enhance power factor, while series capacitor banks are utilized to augment and boost voltage levels by balancing the inductive components. This approach is imperative for safeguarding against overvoltage occurrences resulting from line reactance.

2) *Half Load without reactors*: During half-load operation across all buses, it is observed that voltage levels tend to exhibit higher values compared to the minimum load mode. However, it is essential to note that in the absence of any reactor connections during half-load conditions, certain stations experience elevated voltage levels that surpass the permissible limits. This phenomenon is particularly

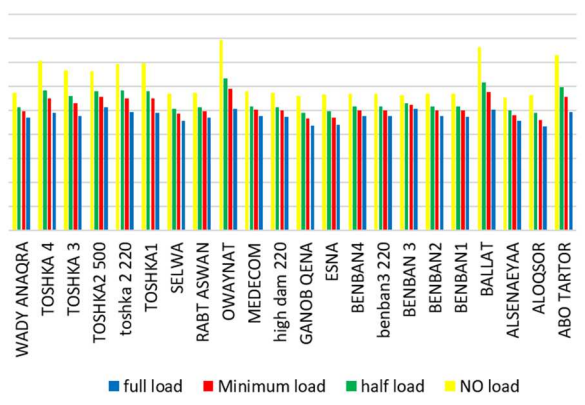


Fig. 3. Various loading scenarios in the absence of reactor connections.

noticeable in stations such as Abo Tartor, Ballat, Owaynat, Toshka1, Toshka 2 220, and Toshka 4.

3) *Minimim Load (65%)*: During the minimum load mode, which corresponds to approximately 65% of the full load operation, notably high voltage values are observed at Balat and Owaynat buses, registering at 115.42 and 117.91, respectively. Similarly, Abo Tartor and Toshka2 500 buses exhibit voltage readings of 111.6 and 112.3, respectively. These findings indicate that at these specific stations, there is a requirement to connect reactors to effectively regulate and fine-tune the voltage levels.

4) *No load condition*: In the absence of load, particular attention is drawn to the exceptionally high voltage levels observed. These voltage readings reach remarkably elevated values, which have the potential to cause extensive damage to the entire system. Consequently, it is imperative to establish reactor connections to mitigate these excessive voltage levels by absorbing the surplus reactive power. This is especially critical as nearly all stations exhibit exceptionally high voltage conditions.

#### B. Reactor Computation in Load Flow Analysis

In ensuring the stable operation of a power system in its steady state, it is imperative that the 'mismatch power equations' which define the relationship between active and reactive power generation, load, and the power exchanged via the transmission elements connecting the buses, collectively sum up to zero. Equations (1) and (2) govern the determination of active and reactive power at bus-k.

$$P_{Gk} - P_{Lk} - \sum_{i=1}^n P_k^{ical} = 0 \quad (1)$$

$$Q_{Gk} - Q_{Lk} - \sum_{i=1}^n Q_k^{ical} = 0 \quad (2)$$

where  $P_{Gk}$ ,  $Q_{Gk}$  are the active and reactive power generations, and  $P_{Lk}$ ,  $Q_{Lk}$  are the active and reactive power of the load connected to bus-k. While  $P_k^{ical}$ ,  $Q_k^{ical}$  are the active and reactive power flow between bus-k and bus-i of the network and can be calculated using (3) and (4).

$$P_k^{ical} = \sum_{i=1}^n V_k^2 G_{ki} + V_k V_i [G_{ki} \cos(\theta_k - \theta_i) + B_{ki} \sin(\theta_k - \theta_i)] \quad (3)$$

$$Q_k^{ical} = \sum_{i=1}^n -V_k^2 B_{ki} + V_k V_i [G_{ki} \cos(\theta_k - \theta_i) - B_{ki} \sin(\theta_k - \theta_i)] \quad (4)$$

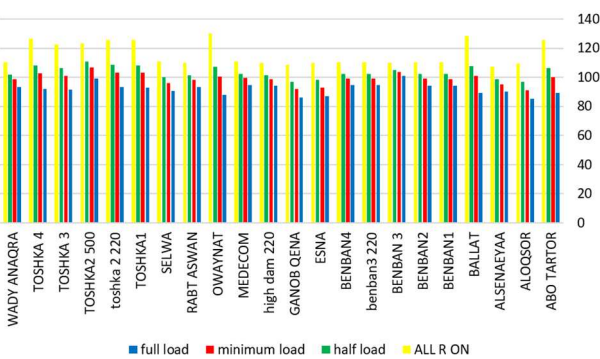


Fig. 4. Various loading scenarios with all reactors connections.

By effectively coordinating reactor control, it becomes possible to continuously adjust the VAR output. The reactor is capable of absorbing reactive power in accordance with the system's voltage levels. Consequently, the reactor functions as a static compensator, regulating the power system's voltage by modulating its reactive drawn current given by (5). And the reactor's reactive power absorbed at bus-k is given by (6).

$$I_R = jB_R V_k \quad (5)$$

$$Q_R = Q_k = -V_k^2 B_R \quad (6)$$

The reactor's susceptance  $B_R$ , required to maintain the bus voltage  $V_k$  at its acceptable value, is iteratively computed using the linearized equation given in (7) and (8).

$$\begin{bmatrix} \Delta P_k \\ \Delta Q_k \end{bmatrix}^{(i)} = \begin{bmatrix} 0 & 0 \\ 0 & Q_k \end{bmatrix}^{(i)} \begin{bmatrix} \Delta \theta_k \\ \Delta B_R / B_R \end{bmatrix}^{(i)} \quad (7)$$

$$B_R^{(i)} = B_R^{(i-1)} + \left( \frac{\Delta B_R}{B_R} \right)^{(i)} \times B_R^{(i-1)} \quad (8)$$

#### C. Operation Modes with All Reactors Connected.

Different loading conditions are simulated with all reactors as shown in Fig. 4 and analyzed as follows:

1) *Full load with all reactors*: In the context of full-load operation, certain stations such as Abo Tartor, Aloqsor, Balat, Esna, Ganob Qena, and Owaynat exhibit lower voltage values, indicating that the inclusion of reactors during full load conditions leads to a reduction in voltage levels. Consequently, there arises a need to consider the removal of reactors in these specific stations. A comparison to the full load scenario reveals that in the absence of reactors, Owaynat's voltage stands at 101.83%, while Ballat records a voltage of 101.11%. However, with reactors in place, Owaynat's voltage drops to 87.91%, and Ballat's voltage decreases to 89.32%. This comparison highlights that during full-load operation, reactor installation is unnecessary, and their removal may be warranted in stations experiencing lower voltage levels.

2) *Half Load with all reactors*: In the scenario of half load with all reactors connected, the values in the table indicate the essential nature of reactor connections to prevent voltage surges. Additionally, specific stations highlighted in the figure require the addition of capacitors to raise their voltage levels without introducing any adverse effects on the system.

3) *Minimum Load with all reactors*: During the minimum load scenario with all reactors activated, it is evident that the voltage levels at all busbars remain within the 100% limit of their rated values. Nevertheless, certain stations, as depicted in the figure, exhibit lower busbar voltage readings. In such instances, the connection of capacitors becomes necessary to elevate these voltage values, ensuring that they do not adversely impact the system.

4) *No-load with all reactors*: In the scenario of no load with all reactors connected, it is noteworthy that despite the connection of all reactors, the voltage levels continue to remain at exceptionally high values, posing a significant challenge.

#### D. Future Load Projections

From Fig. 5, it is observed that an increase in loading results in a more substantial decrease in voltage levels, particularly when reactors are actively employed. As a consequence, the necessity for additional reactor installations in the future does not appear to be warranted. A 5% increase in loading leads to voltage reduction in stations such as Abo Tartner, Aloqsor, Alsenaeayaa, Balat, Esna, Ganob Qena, Owainat, and Selwa. With a 10% loading increment, voltage drops are observed in the same stations, including Toshka3 and Toshka4. Moreover, with a 15% increase in loading, voltage reductions are noted in the previously mentioned stations, as well as in Toshka1, Toshka2 220KV, Toshka3, and Toshka4.

"When considering a 20% future load increase with all reactors in operation, it's clear that voltage decreases occur at specific stations, making additional reactors unnecessary. Importantly, voltage levels are notably lower in these future scenarios compared to when reactors are active. This suggests that, in the absence of reactors, voltage levels remain within an acceptable range. In the future, as loads increase, capacitors may be needed to raise low voltage levels."

#### V. CONCLUSION

This paper presents a comprehensive study on the selection and impact of shunt reactors in high-voltage transmission systems, with a particular focus on interconnected long transmission lines. The contribution of this research lies in its thorough analysis of various operational modes and scenarios, providing valuable insights into the necessity and optimization of reactor deployment. The key findings of this study have significant implications for enhancing the reliability, stability, and cost-effectiveness of power transmission systems.

The findings of this research offer critical guidance for power system engineers and operators:

- In full-load conditions, where all voltages remain within suitable ranges, reactor installation is generally unnecessary. However, during minimum load scenarios, voltage percentages can surge beyond acceptable limits, emphasizing the need for reactor deployment to maintain voltage stability and prevent potential equipment damage.
- Moreover, under half-load and no-load conditions, voltage percentages can reach excessive levels, posing a substantial risk to the system's integrity. Reactor installation is imperative in such cases to limit overvoltage during line energization, load rejection, and light load conditions, safeguarding the system and its components.
- With anticipated load growth, reactor installation may not be warranted as voltage percentages drop significantly. In such instances, considering capacitance installation to compensate for power with load growth becomes a more cost-effective option.
- Furthermore, the existing reactor capacities have been determined to be adequate, eliminating the need for capacity expansion. This decision aligns with

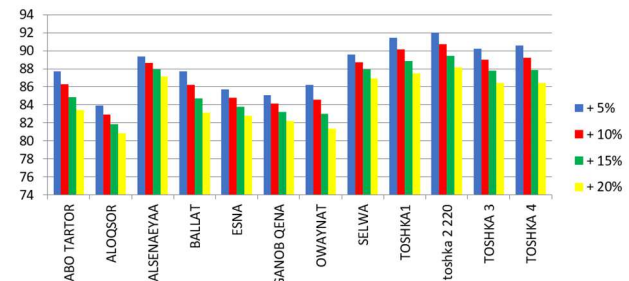


Fig. 5. Anticipated Future Loading with All Reactors Enabled.

enhancing system reliability while managing costs effectively.

- Overall, this research underscores the significance of reactor deployment in optimizing power transmission systems' performance, providing a roadmap for achieving voltage stability and system health under diverse operating conditions.

#### REFERENCES

- [1] O. Oghorada, L. Zhang, A. Esan, D. Egbune, and J. Uwagboe, "Inter-cluster Voltage Balancing Control of Modular Multilevel Cascaded Converter Under Unbalanced Grid Voltage," *Journal of Modern Power Systems and Clean Energy*, vol. 10, no. 2, pp. 515–523, Mar. 2022, doi: 10.35833/MPCE.2019.000129.
- [2] Q. Yang, S. Chen, X. Zeng, G. Wei, H. Liu, and T. Chen, "Suppression Measures for Overvoltage Caused by Vacuum Circuit Breaker Switching off 10-kV Shunt Reactor," *IEEE Transactions on Power Delivery*, vol. 35, no. 2, pp. 540–548, Apr. 2020, doi: 10.1109/TPWRD.2019.2912663.
- [3] M. I. Mosaad and N. A. Sabiha, "Ferroresonance Overvoltage Mitigation Using STATCOM for Grid-connected Wind Energy Conversion Systems," *Journal of Modern Power Systems and Clean Energy*, vol. 10, no. 2, pp. 407–415, Mar. 2022, doi: 10.35833/MPCE.2020.000286.
- [4] A. A. Bhandakkar\* and L. Mathew, "Real-Time Simulation of Static VAR Compensator and Static Synchronous Compensator," *International Journal of Recent Technology and Engineering (IJRTE)*, vol. 8, no. 6, pp. 1950–1958, Mar. 2020, doi: 10.35940/ijrte.F8047.038620.
- [5] C. A. Ordóñez, A. Gómez-Expósito, and J. M. Maza-Ortega, "Series compensation of transmission systems: A literature survey," *Energies*, vol. 14, no. 6. MDPI AG, Mar. 02, 2021. doi: 10.3390/en14061717.
- [6] R. Rashid and K. Tomar, "A Study of Static Var Compensation Using TSC – TCR Shunt Compensator," *International Journal of Innovative Research in Engineering & Management*, pp. 61–68, Feb. 2022, doi: 10.5524/ijirem.2022.9.1.10.
- [7] R. R. Hete, S. K. Mishra, R. Dash, A. Ballaji, V. Subburaj, and K. Jyotheeswara Reddy, "Analysis of DFIG-STATCOM P2P control action using simulated annealing techniques," *Heliyon*, vol. 8, no. 3, Mar. 2022, doi: 10.1016/j.heliyon.2022.e09008.
- [8] K. Mehmood, K. M. Cheema, M. F. Tahir, A. Saleem, and A. H. Milyani, "A comprehensive review on magnetically controllable reactor: Modelling, applications and future prospects," *Energy Reports*, vol. 7. Elsevier Ltd, pp. 2354–2378, Nov. 01, 2021. doi: 10.1016/j.egyr.2021.04.027.
- [9] T. Pham Minh, H. Bui Duc, and V. Dang Quoc, "Analysis of Leakage Inductances in Shunt Reactors: Application to High Voltage Transmission Lines," 2022. [Online]. Available: [www.etasr.com](http://www.etasr.com)
- [10] S. Grebovic, N. Oprasic, and A. Balota, "Influence of Shunt Reactor Switching on Overvoltages in 400 kV Substation," in *Mediterranean Conference On Embedded Computing*, 2020.